engineering proceedings

MDPI

Proceeding Paper

Design of an Electromechanical Testing Machine for Elastomers' Fatigue Characterization †

Gabriel Testa [1], Nicola Bonora [1], Luca Esposito [2] and Gianluca Iannitti [1,*]

[1] Department of Civil and Mechanical Engineering, University of Cassino and Southern Lazio, IT-03043 Cassino, Italy; gabriel.testa@unicas.it (G.T.); bonora@unicas.it (N.B.)
[2] Department of Chemical, Materials and Production Engineering, University of Naples Federico II, IT-80125 Napoli, Italy; luca.esposito2@unina.it
* Correspondence: g.iannitti@unicas.it
† Presented at the 53rd Conference of the Italian Scientific Society of Mechanical Engineering Design (AIAS 2024), Naples, Italy, 4–7 September 2024.

Abstract: The VITAL-E (Versatile Innovative Testing Low-Cycle Fatigue for Elastomers) project introduces a shift in low-cycle fatigue (LCF) testing by replacing traditional hydraulic systems with an electromechanical solution. Hydraulic machines, although widely used, present issues such as fluid leakage, environmental impact, high maintenance, and complex feedback control. In contrast, VITAL-E incorporates a zero-backlash linear actuator, addressing a key challenge in electromechanical systems: backlash. This issue, caused by axial movement between the nut and screw during load reversals, can disrupt load application and compromise test accuracy. By eliminating backlash, the chosen actuator ensures continuous and precise load application, especially during critical cycle reversals, enhancing both the accuracy and reliability of LCF testing. Beyond technical improvements, the electromechanical system reduces component complexity, wear, and maintenance needs while offering easier upgrades and adaptability to evolving testing demands. Compared to conventional hydraulic systems, VITAL-E's design offers an innovative industrial solution, promoting a new generation of LCF test machines that excel in accuracy, reliability, and operational efficiency. This innovation aligns with the growing demand for sustainable and adaptable testing solutions, particularly in the automotive industry, ensuring that LCF testing remains relevant for future research and industrial needs.

Keywords: low-cycle fatigue; elastomers; inverted roller screw

Academic Editors: Umberto Galietti, Gabriele Arcidiacono, Enrico Armentani, Davide Castagnetti, Vigilio Fontanari and Aurelio Somà

Published: 19 February 2025

Citation: Testa, G.; Bonora, N.; Esposito, L.; Iannitti, G. Design of an Electromechanical Testing Machine for Elastomers' Fatigue Characterization. *Eng. Proc.* **2025**, *85*, 21. https://doi.org/10.3390/engproc2025085021

1. Introduction

Mechanical components are subject to various failure mechanisms depending on their application. Some of the main failure mechanisms are as follows:

- Plastic collapse, which can occur under quasi-static stresses [1–4] or under dynamic conditions like high-velocity impacts [5–7];
- Creep, where long-term exposure to high temperatures and external stress are the key factors [8–10];
- Brittle fracture, driven by the nucleation, growth, and propagation of cracks due to maximum principal stress, which leads to the opening of material defects [11–13].

In addition to these failure mechanisms, fatigue failure, although known as early as the late 19th century [14,15], is still the focus of significant industry and academic research due to the impossibility of precisely predicting the instant at which the material will fail under operating conditions [16–18] and historically, fatigue failures have often

been the cause of catastrophic events [19,20]. For these reasons, it is important to define accurate characterization plans for materials, depending on the loading conditions to which they will be subjected. In modern fatigue testing, different loads can be applied (axial, bending, torsional, or combinations thereof) that aim to determine the number of cycles a material can endure before failure, depending on the applied strain/stress levels and loading conditions. Electromechanical machines are mainly used for bending loads and are based on R.R. Moore's high-speed rotating beam machine, while hydraulic systems are still dominant for axial loads [21–23]. Although hydraulic machines are well-established, they pose environmental concerns due to the need for hydraulic fluids and cooling systems. Environmental and sustainability factors are critical in mechanical design today, as the Next-Generation EU (NGEU) program emphasizes.

Recently, the leading manufacturers of testing machines, like Instron, MTS, Shimadzu, and Zwick Roell, have started to produce new fatigue devices, including electromechanical ones. In their products, an electrodynamic actuator, based on linear motor technology, is employed. Although this solution allows for high frequencies of up to 100 Hz, it has drawbacks, such as high costs, limited crosshead strokes of less than 100 mm, and reduced load capacity at high frequencies. In fact, at high velocities, the maximum load of the linear motor is only sufficient to move itself due to its high weight. However, the device's management software, while compliant with current characterization testing standards, does not allow users to implement additional test configurations. Several home-built electromechanical devices have been proposed in the literature to perform fatigue tests, mainly based on R.R. Moore's scheme [24–29], or to carry out high-frequency bending tests [30]. To overcome these limitations, an innovative fatigue machine was designed using funds from the Italian National Recovery and Resilience Plan (PNRR) program. The VITAL-E (Versatile Innovative Testing Low-Cycle Fatigue for Elastomers) project aimed to design an electromechanical device for the low-cycle fatigue characterization of different classes of materials. The project was funded by the Closed Call for Proof of Concept initiative issued by the MOST (Sustainable Mobility) HUB. The mission of MOST is to make mobility greener as a whole and more digital in its management through lightweight solutions, electric and hydrogen propulsion systems, digital systems for accident reduction, more effective solutions for public transport and logistics, and a new, accessible, and inclusive mobility model. The various areas of focus also include the characterization of new elastomeric materials [31] together with the modeling of both the mechanical behavior and prediction of the fatigue life of such materials used to manufacture innovative tires and safety devices [32]. When focusing on rubber materials, which play a central role in the automotive industry, it is of utmost importance to characterize and understand their response under cyclic loading across a wide range of frequencies, since this is the predominant failure mode in operative conditions [33,34]. From this perspective, understanding fatigue failure can provide new insights for optimizing tire design, providing MOST partners with innovative tools to successfully achieve their research goals. In this paper, the design of a cost-effective low-cycle fatigue (LCF) machine, based on commercially and industrially available components, is presented. The main goal is to develop a multipurpose, low-cost machine for testing elastomers and other materials of interest to MOST partners and to give users the ability to customize the testing machine software.

2. Materials and Methods

The design of the fatigue testing machine was developed using Computer-Aided Design (CAD) software. This type of software is helpful for developing parametric 3D models and includes several environments such as those used for kinematic, static, and dynamic structural analysis. These tools enable the design of complex systems, incorporating all

parts without simplification. In addition, it is possible to analyze different configurations and optimize each component's design to meet the project's goal. However, these tools have some limitations; for example, they cannot perform elastoplastic analysis and support only tetrahedron elements.

Design Specifications and Machine Layout Conceptualization

The goal of the project was to design a testing machine specialized for LCF tests, with the following design parameters:

- Maximum load of 50 kN;
- Maximum load frequency 10 Hz;
- Capability to perform fatigue tests with $R < 0$;
- The device's control system must be robust and open access to allow customization to meet MOST partners' needs;
- High specimen dimension scalability;
- Reduction of the device's environmental impact compared to traditional hydraulic systems.

To meet all these requirements, conventional hydraulic systems, despite being widely used for their high performance, are not a viable solution, particularly for reducing environmental impact, which is one of the critical issues addressed by MOST. On the other hand, classical electromechanical machines are too slow compared to their hydraulic counterparts and are unsuitable for load inversion. A possible solution to meet the design requirements is the implementation of a jack. This type of linear actuator converts the rotational motion of an electrical motor into linear motion using a leadscrew. There are several types of linear actuators commercially available, and they differ depending on the leadscrew system used:

- Trapezoidal leadscrew, Figure 1a;
- Ball screw, Figure 1b;
- Planetary roller screw, Figure 1c;
- Recirculating roller screw, Figure 1d.

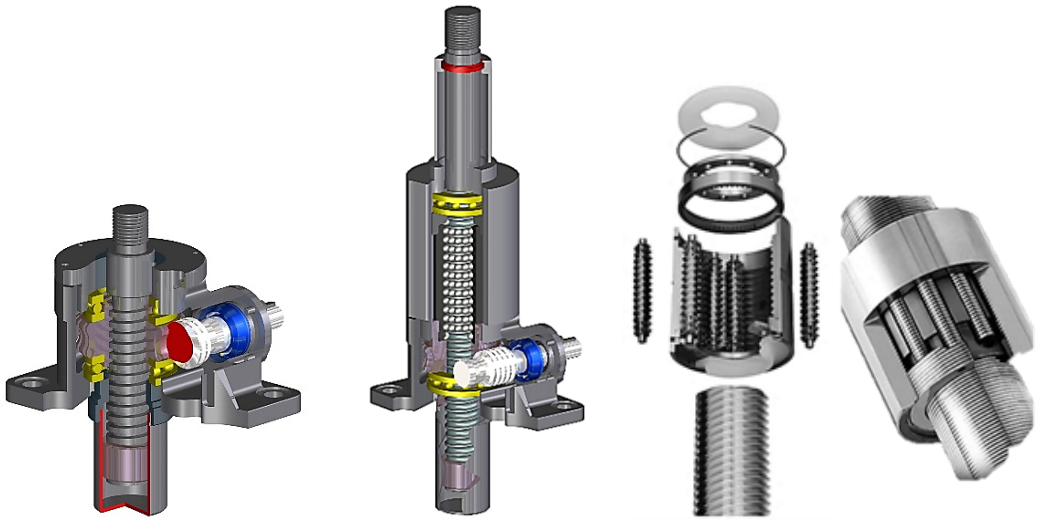

(**a**) (**b**) (**c**) (**d**)

Figure 1. Examples of leadscrew for jacks: (**a**) Trapezoidal leadscrew. (**b**) Ball screw. (**c**) Inverted roller screw. (**d**) Recirculating roller screw.

The first type, the trapezoidal screw, is mainly used for cheaper applications (which generally require low axial velocity) but is characterized by high friction and high backlash, i.e., the axial distance between the two parallel faces of the threads of the nut and screw, which causes a discontinuity in the applied load during reversal. During load-sign

inversion, the sample is not subjected to external load until the threads of the nut and screw come into contact again. The other three screw types were mainly developed to reduce friction between the nut and the screw by interposing an element such as a ball (ball screw) or roller (inverted or recirculating ball screw). Furthermore, in these types of screws, backlash can be reduced or eliminated by preloading the rolling elements within the system. The main differences between a ball screw and a roller screw are their maximum velocity and load capacity. The former is used in high-speed applications, while the latter is used in high-load applications. In addition, the roller screw generally has a smaller pitch than the ball screw, making it more suitable for applications requiring small axial displacements with high accuracy, and it meets the performance requirements for this application.

The frame of fatigue machines is generally designed to enhance both stiffness and natural frequency:

- The former is necessary to minimize the machine's elastic deformation contribution to the total stroke displacement, thereby reducing measurement errors in the specimen's strain and improving feedback control response.
- The latter significantly impacts the resonance frequency of the machine; therefore, the natural frequency of the frame should be greater than the maximum design frequency.

The frame was designed to reduce compliance and maximize weight to meet the design goal. It consists of the following:

- A bottom plate, where the jack and four columns are bolted;
- A top plate, where a synchronous belt system is installed to move the middle plate and lock the four columns;
- A middle or moving plate, where the load cell, alignment system, and top grip are installed. Furthermore, the middle plate is adjustable to accommodate different specimen lengths.

The frame is assembled on a base, made of structural beams, providing sufficient space to install the jack below the frame. This solution lowers the device's center of gravity and helps prevent unwanted oscillations at its operating frequency.

3. Design of Fatigue Testing Machine

3.1. Linear Actuator Selection

When performing fatigue tests, the load application system may experience a sign reversal depending on the selected load ratio parameter ($R = P_{min}/P_{max}$). During the reversal, the specimen shifts from a tensile to a compressive stress state, and if there is any backlash in the load application system, there will be a period of time when the specimen does not experience any loading. Traditional fatigue testing machines use hydraulic actuators, which have no backlash but are expensive to purchase, maintain, and operate. Additionally, they have a significant environmental impact due to the periodic disposal of spent hydraulic oil and high energy consumption, especially if they do not have an adjustable flow rate pump. To overcome these issues, jacks employing rolling elements provide a valid solution. Actuators with recirculating ball screws may not be suitable due to low wear resistance and high pressure in the ball–screw contact. Thorough market research indicates that inverted roller screw jacks are more suitable for specific purposes. These jacks have many advantages, such as reduced pitch, the ability to apply high loads (15× that of ball screws), reduced clearance between the screw and nut, and long component lifetimes (2× that of ball screws). However, these technological advantages come at a higher cost, approximately 10× that of a ball screw jack with the same load capacity. Figure 2a shows a planetary inverted rolled screw system as an example. Many companies manufacture this type of linear actuator but it is not yet common, which makes procurement difficult,

especially when buying small quantities. The FTX 125 linear actuator, made by EXLAR and illustrated in Figure 2b, was selected for this specific application, and its main operating parameters are listed in Table 1.

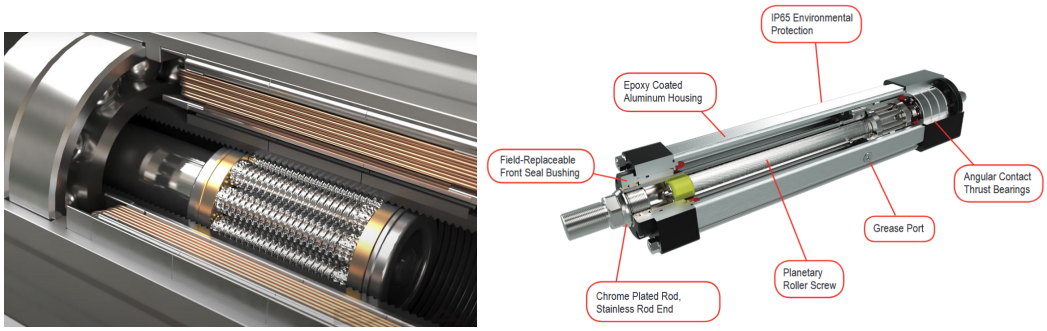

(**a**) (**b**)

Figure 2. (**a**) Examples of main elements of planetary inverted roller screw. (**b**) FTX 125 planetary inverted roller screw by EXLAR.

Table 1. Main data of the FTX 125 linear actuator from EXLAR.

Dimension	Unit	Value
Maximum deviation on stroke	mm	0.03
Maximum screw pitch error	mm/300 mm	0.025
Maximum clearance between the screw and nut (backlash)	mm	0.03
Maximum dynamic load	kN	44.5
Screw pitch	mm	5
Life	km	249.2
Maximum linear velocity	mm/s	292

During load reversal, the specimen may remain unstressed for very short periods due to the small clearance between the screw and nut, which is less than 0.03 mm. The duration of this time depends on the size of the test specimen and the level of strain applied during the test. Figure 3 outlines the specimen sizes specified in ASTM D4482. According to this standard, the length of the calibrated section, in which a uniform stress and deformation state is experienced by the material, is 25 mm. With a strain amplitude of 0.005 mm/mm during the test, the displacement of the specimen head will be at least $\pm$0.03 mm, which is equal to the maximum backlash of the chosen linear actuator. In this case, the maximum time the specimen is unstressed corresponds to the cycle time. However, it is essential to note that during the experimental test, the displacement of the driven grip will exceed that of the calibrated section of the specimen. In addition to the gauge section, the connecting radii and the portion of the specimen heads that are not within the grips will also undergo deformation, and inevitable deformation of the frame will also occur. The strain amplitude assumed above represents the lower bound for low-cycle fatigue tests on elastomers, which require significantly larger stress/strain amplitudes.

The frame's lower part houses the linear actuator, which is installed in the "FRONT FLANGE" configuration (Figure 4a). The brushless motor is mounted parallel to the actuator, as illustrated in Figure 4b. This arrangement was primarily chosen to keep the jack's total length within acceptable limits, as an inline motor would have significantly increased its length. The constraint on the jack's length also influenced the choice of stroke, which, in this case, is 150 mm, making it suitable for the machine's design.

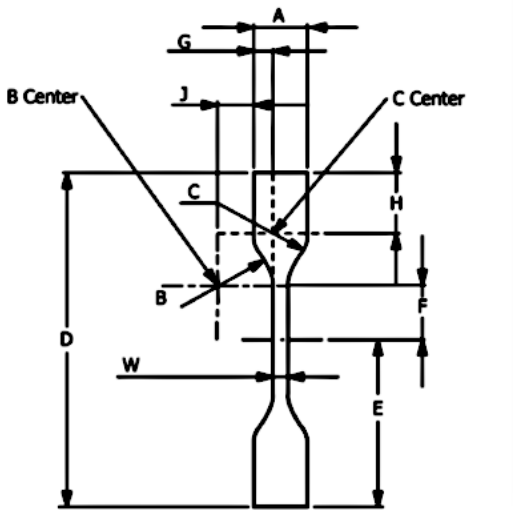

	mm	in.
A	12.50 ± 1.00	0.492 ± 0.039
B	12.50 ± 0.030 R	0.492 ± 0.012 R
C	8.00 ± 0.030 R	0.315 ± 0.012 R
D	78.74 ± 0.013	3.100 ± 0.005
E	39.37 ± 0.064	1.550 ± 0.0025
F	12.50 ± 0.25	0.492 ± 0.010
G	4.50 ± 0.050	1.770 ± 0.020
H	14.39 ± 0.050	0.5664 ± 0.02
J	8.26 ± 0.050	0.3250 ± 0.02
W	4.01 + 0.05/−0.00	0.1580 + 0.002/− 0.000

Figure 3. Smooth specimen sizes specified in ASTM D44882.

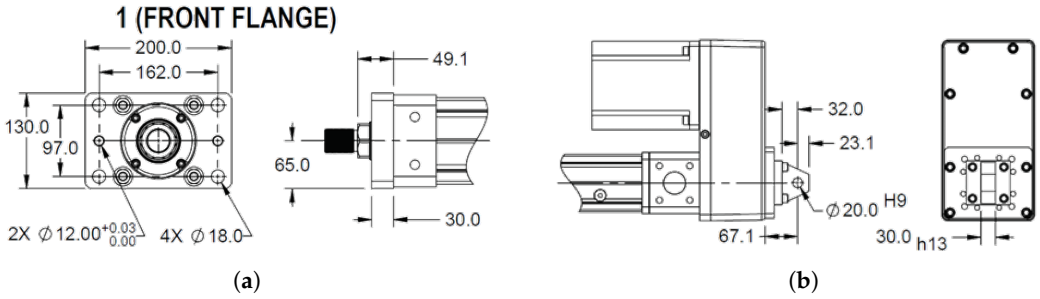

Figure 4. Technical details of the EXLAR FTX 125: (**a**) Front flange. (**b**) Motor configuration.

3.2. Frame Design

The frame was designed to meet the requirements of both overall external and internal space dimensions, which are necessary to ensure that all accessories are installed correctly and the user has enough space to work safely. To facilitate easy movement of the machine within test laboratories, the maximum size was chosen to allow the device to fit through standard doorways by disassembling only a few parts. Handling can be accomplished using a pallet truck that lifts the frame through bars positioned higher than the pallet truck's forks. The machine's width was kept within 70 cm, which is a typical doorway width. The spacing between the columns was designed to accommodate a classic muffle furnace and a mobile radio-frequency (RF) heater unit. The spacing between the columns is 530 mm. Figure 5 shows a 3D model of the LCF machine.

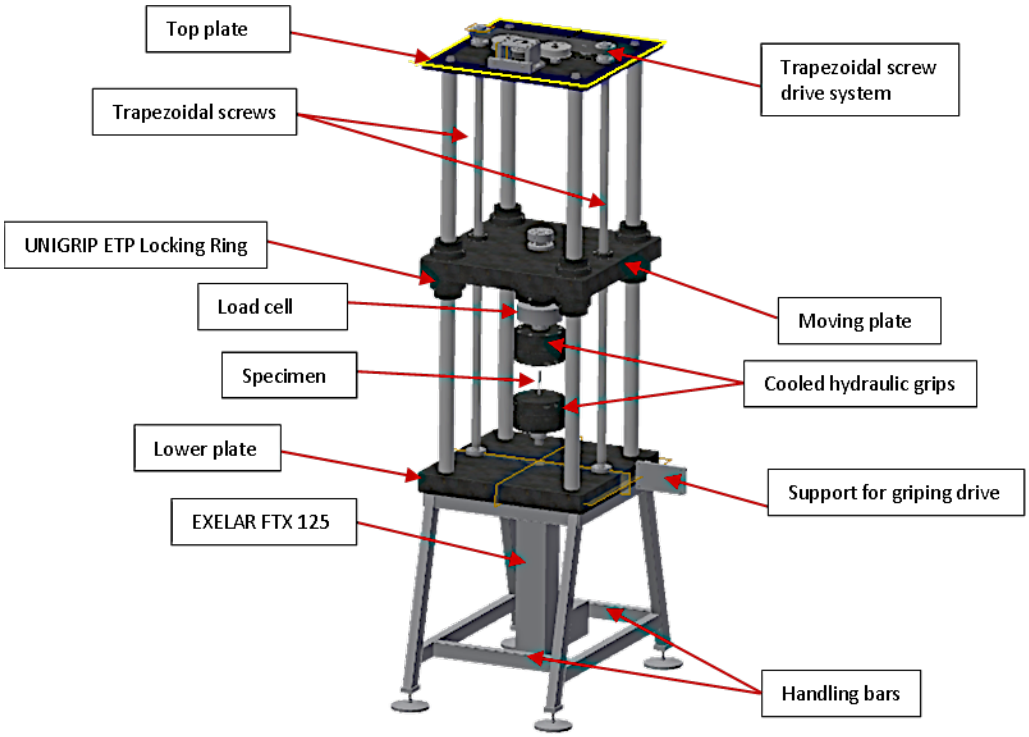

Figure 5. Three-dimensional model of the LCF machine.

The machine comprises three plates: a bottom plate, a top plate, and a moving plate. The latter is driven by two trapezoidal screws, which are powered by a gear motor via a synchronous belt drive system. The pulleys are attached to the trapezoidal screws using ETP Classic 24 locking bushings, as shown in Figure 6b. The use of these bushings is crucial for several reasons:

- They ensure that the moving plate remains perfectly parallel to the bottom plate during assembly by allowing individual actuation of the trapezoidal screws.
- They prevent the pulleys from slipping on the corresponding screws.
- They reduce the overall dimensions of the toothed pulleys.
- They facilitate the installation and removal of the timing belts.
- The drive pulley is connected to the stepper motor through a single-stage gearbox with an 8:1 reduction ratio, as shown in Figure 6a.

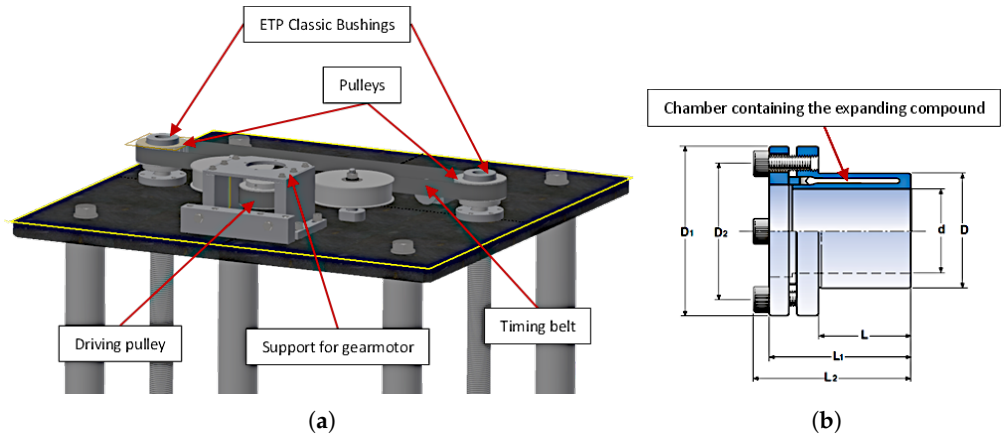

(**a**) (**b**)

Figure 6. Details of the system for moving the middle plate: (**a**) Details of the moving plate drive system. (**b**) Drawing of the ETP Classic bushing.

The moving plate is kept in place by four linear recirculating roller bearings from SKF, which are positioned inside the four holes made on the plate to allow the columns to pass through. These bearings are essential to prevent the plate from snagging on the columns and causing damage to the fixed and moving parts. After being positioned at the correct distance from the bottom plate, the moving plate is locked in place using eight UNIGRIP ETP bushings arranged on the top and bottom of the plate and for each of the columns, as shown in Figure 7a. These bushings have three axial plungers, as shown in Figure 7b, which allow them to apply an 80 kN preload on the moving plate (20 kN for each), about twice the jack's maximum load. The ETP UNIGRIP bushings can radially clamp around the column, and their axial plungers can apply a preload on the moving plate, which helps reduce the compliance of the machine. The dimensions of the structural elements were determined through finite element analysis. The system must operate in the linear-elastic regime, but because of the complexity of the geometry and contact elements, a classical design approach would be too coarse. Therefore, several configurations, with different column diameters and thicknesses of the bottom and moving plates, were analyzed. The first solution, used as a reference, had a thickness of 40 mm for both the bottom and moving plates and a column diameter of 60 mm. The second configuration involved increasing the plate thickness from 40 mm to 78 mm and decreasing the column diameter from 60 mm to 40 mm. The third configuration had 78 mm plates and 60 mm diameter columns. The last configuration, as displayed in Figure 8, started with the dimensions analyzed in the second configuration. However, the moving plate consisted of two 25 mm-thick plates spaced 100 mm apart, using two webs aligned along the diagonals of the plates. The dimensions of the most stressed components are summarized in Table 2. For all solutions, plates and structural elements were designed assuming S235JR steel, with yields and ultimate tensile strengths of 235 MPa and 340 MPa, respectively, while the columns, on which various elements, including recirculating ball bearings, run, were made of 304 stainless steel, with yields and ultimate tensile strengths of 215 MPa and 505 MPa, respectively.

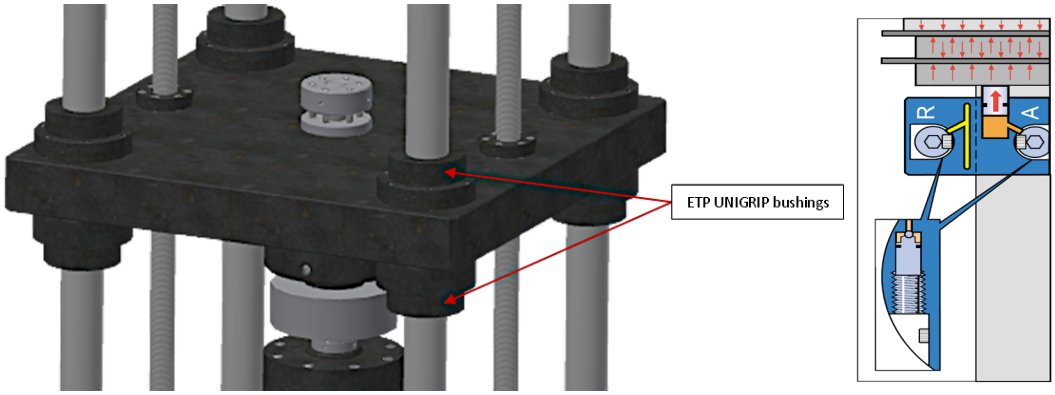

(**a**) (**b**)

Figure 7. (**a**) Details of the system for locking the middle plate. (**b**) Details of the axial locking bushing.

Two types of structural analysis were performed. A quasi-static analysis of the four solutions was performed to assess the stiffness of the main components under stress during the tests: the horizontal plates and the four columns. In all cases, a maximum simulated load of 50 kN was applied to the moving plate. All displacements were constrained at the central hole present in the bottom plate. For all configurations, the distance between the bottom and moving plates was set to 370 mm in order to assess compliance under the most critical conditions.

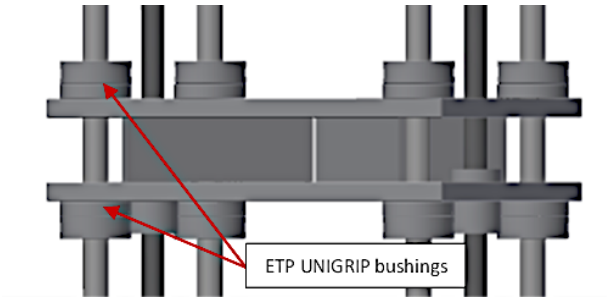

Figure 8. Details of the moving plate for Solution 4.

Table 2. Dimensions of the most stressed components in the analyzed solutions.

Configuration	Moving-Plate Thickness (mm)	Bottom-Plate Thickness (mm)	Column Diameter (mm)
Solution 1	40	40	40
Solution 2	78	78	40
Solution 3	78	78	60
Solution 4	78	25 × 2	40

Then, a modal analysis of the optimum configuration was performed to determine the inherent dynamic characteristics of the system, ensuring that the natural frequency of the fatigue machine did not match the test frequency. For this type of analysis, it is crucial to accurately account for the overall mass and stiffness of the structure to identify the periods at which it will naturally resonate. For this reason, all components were included in the modal analysis. In this case, all displacements of leveling feet with vibration-damping elements were fixed.

After developing the computational model, the software automatically identified the contact interaction between the different parts and generated computational grids based on the tetrahedron elements.

4. Results and Discussion

4.1. Quasi-Static Analysis Results

Table 3 summarizes the numerical results obtained for the investigated solutions. The most critical conditions were found for Solution 1, where the maximum equivalent stress calculated exceeded the material yield stress (235 MPa). For the other solutions, the equivalent stress computed was within the elastic limit. By looking at the total plate deflection, i.e., the sum of the deflections of both plates, it was observed that increasing the thickness of the plates made the frame stiffer. This was confirmed by Solution 2, which had a maximum total deflection of 0.15 mm, compared to 0.54 mm for Solution 1. Increasing the size of the columns had a minimal impact on frame stiffness. In fact, Solution 3 had a total deflection of 0.125 mm, which was 0.025 mm less than that of Solution 2. Finally, Solution 4 was implemented to reduce the weights of the plates by increasing the moment of inertia of the moving plate. Despite the 40 mm columns, using two 25 mm plates spaced with two cores 10 mm thick and 100 mm high, the maximum deflection obtained was 0.13 mm. This confirms what was stated earlier about the impact of plate thickness; in fact, Solution 4 had a deflection only 0.005 mm greater than that of Solution 3 and 0.02 mm lower than that of Solution 2. However, Solution 4 had greater construction complexity.

Figure 9a,b show the fringes of the displacement and the equivalent von Mises stress, respectively, for Solution 3, which offered the best compromise between stiffness and simplicity.

Table 3. Summary of results obtained through numerical simulation by applying a static force of 50 kN.

Configuration	Maximum von Mises Stress (MPa)	Difference (%)	Total Plate Deflection (mm)	Difference (%)
Solution 1	266	-	0.542	-
Solution 2	97	63.53	0.149	73
Solution 3	31	88	0.125	77
Solution 4	115	57	0.131	76

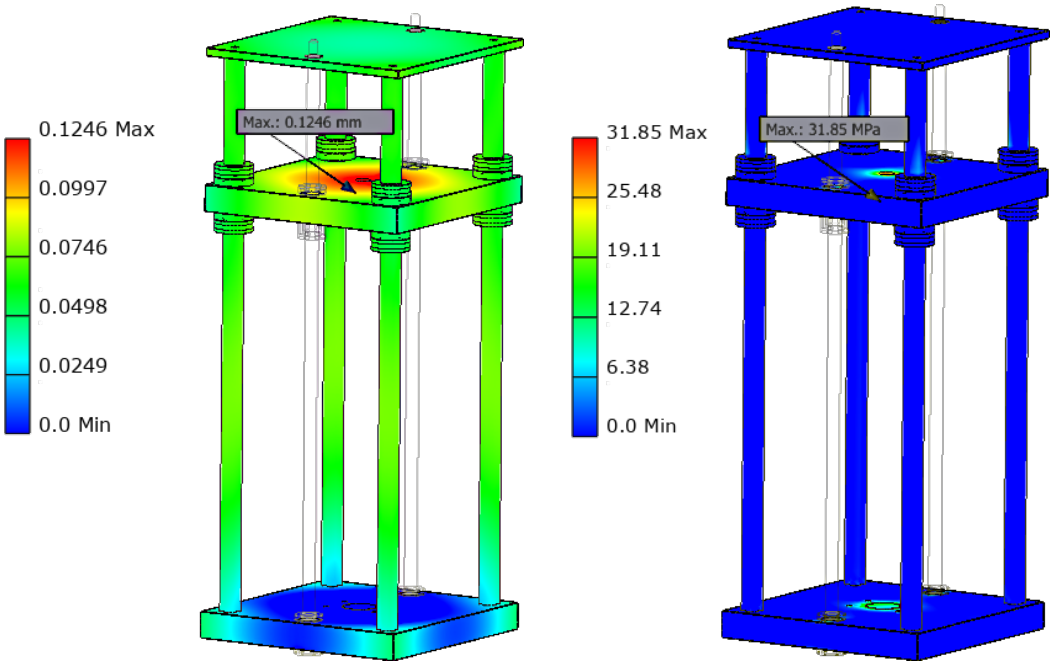

Figure 9. Fringes for Solution 3: (**a**) Displacement and (**b**) equivalent von Mises stress.

4.2. Modal Analysis Results

Modal analysis was performed on Solution 3 to determine the natural frequency of resonance by evaluating the first twelve modes. Figure 10 shows in the wireframe view the original shape and the frame's deformation obtained through the modal analysis for the lowest frequency and for the vibration mode that deforms the frame similarly to the load applied by the jack. Based on the frame deformation shown in Figure 10a, the first mode had a resonance frequency of 9.3 Hz, but this was associated with an external load applied to the base of the frame that bent the device like a cantilever beam. During the tests, the frame was stressed with a load applied in the vertical direction. The mode associated with this deformation is shown in Figure 10b and was characterized by a natural frequency of 106.7 Hz. This large value is related to the greater axial stiffness compared to the flexural stiffness of the designed machine. Therefore, no adjustments are needed to avoid resonance phenomena.

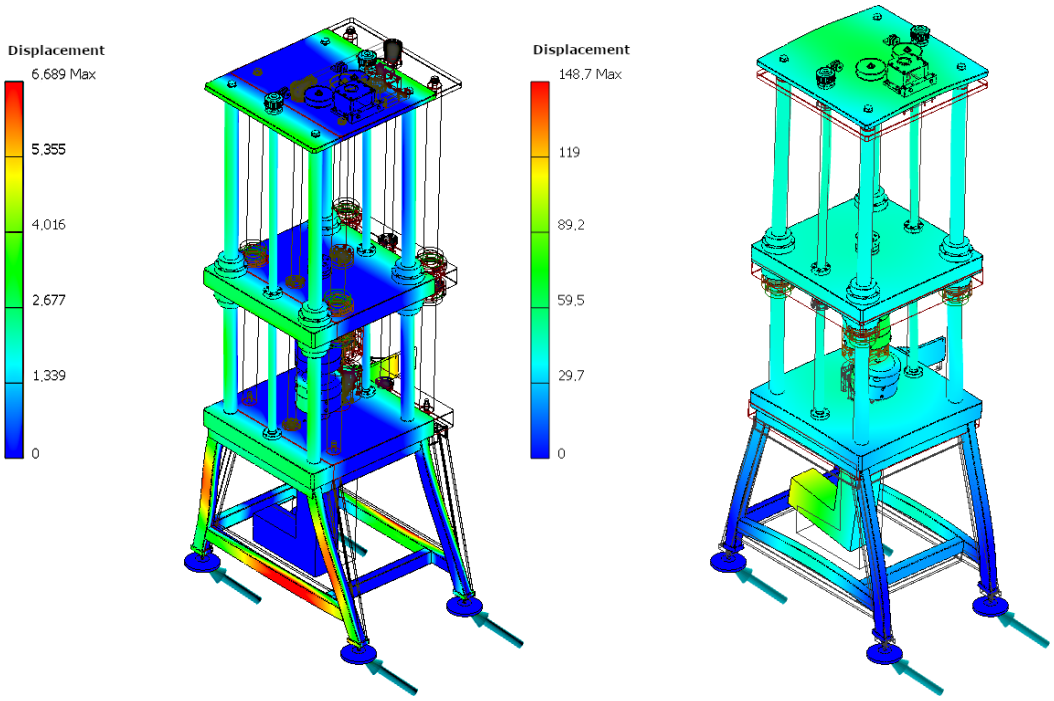

(**a**) (**b**)

Figure 10. Modal analysis results: (**a**) Frame deformation related to the first mode. (**b**) Frame deformation related to the twelfth mode.

5. Conclusions

A fatigue machine was designed by developing a complete, high-fidelity virtual model with Computer-Aided Design software. The device was developed to conduct tests with a maximum load of 50 kN at a maximum frequency of 10 Hz. The main frame is characterized by three plates. Below the bottom plate, there is a commercial inverted roller screw jack that applies cyclic load, while on the opposite side, there are four smooth columns and two trapezoidal screws. The selected linear actuator offers several advantages over other solutions, such as a reduced pitch, the ability to apply high loads (15× that of ball screws), minimal clearance between the screw and nut, and long component lifetimes (2× that of ball screws). However, these technological advantages come at a higher cost of approximately 10× that of a ball screw jack with the same load capacity. The columns are locked at the top by a plate, on which a synchronous belt system is mounted to drive the moving plate through the trapezoidal screws. The load cell and the other specimen grip are installed on the moving plate. To increase stiffness, during the tests, the moving plate is constrained on the four columns through hydraulic bushes that enable the preloading of the moving plate with a maximum load of 80 kN.

All frame components were designed using finite element analysis with the aim of reducing frame compliance and avoiding coupling between the natural resonance frequency and the test frequency. Several configurations were investigated by applying a maximum load of 50 kN. This analysis showed that stiffness is influenced more by plate thickness than by column diameter. Then, for the selected configuration, characterized by greater stiffness and simplicity of fabrication, modal analysis was performed to determine the natural resonance frequency. With the results of the analysis, the first twelve vibration modes of the frame were determined, and only the last one, with a frequency of 106.7 Hz, was characterized by a frame deformation akin to that induced by the jack. Finally, a prototype of the machine was built, which is in the validation phase and will be available to all MOST partners.

VITAL-E may represent a significant innovation in low-cycle fatigue (LCF) testing by offering a cost-effective electromechanical solution with lower maintenance costs and a longer lifetime compared to traditional machines. This solution makes it particularly attractive for research institutions, manufacturing companies, and laboratories looking for more durable and cost-effective testing options. Furthermore, the machine's compact design and operational versatility make it suitable for both small laboratory environments and larger industrial environments. The integration of customizable software makes VITAL-E an ideal tool for researchers requiring flexible test scenarios.

Author Contributions: Conceptualization, G.T. and L.E.; methodology, G.T. and N.B.; software, G.T.; validation, G.I.; formal analysis, G.T. and L.E.; writing—original draft preparation, G.I. and G.T.; writing—review and editing, G.T. and G.I. visualization, L.E.; supervision, N.B.; project administration, G.T. and L.E.; funding acquisition, N.B. All authors have read and agreed to the published version of the manuscript.

Funding: This study was carried out within the MOST (Sustainable Mobility) HUB and received funding from the European Union Next-Generation EU (PIANO NAZIONALE DI RIPRESA E RESILIENZA (PNRR)—MISSIONE 4 COMPONENTE 2, INVESTIMENTO 1.4—D.D. 1033 17/06/2022, CN00000023). This manuscript reflects only the authors' views and opinions; neither the European Union nor the European Commission can be considered responsible for them.

Institutional Review Board Statement: Not applicable.

Informed Consent Statement: Not applicable.

Data Availability Statement: No new data were created or analyzed in this study. Data sharing is not applicable to this article.

Conflicts of Interest: The authors declare no conflicts of interest. The funders had no role in the design of the study; in the collection, analyses, or interpretation of data; in the writing of the manuscript; or in the decision to publish the results.

References

1. Ricci, S.; Zucca, G.; Iannitti, G.; Ruggiero, A.; Sgambetterra, M.; Rizzi, G.; Bonora, N.; Testa, G. Characterization of Asymmetric and Anisotropic Plastic Flow of L-PBF AlSi10Mg. *Exp. Mech.* **2023**, *63*, 1409–1425. [CrossRef]
2. Testa, G.; Ricci, S.; Iannitti, G.; Ruggiero, A.; Bonora, N. Modeling ductile fracture in third stress invariant sensitive materials: Application to Al 2024-T351. *Mech. Mater.* **2023**, *179*, 104584. [CrossRef]
3. Ricci, S.; Iannitti, G. Mechanical Behavior of Additive Manufacturing (AM) and Wrought Ti6Al4V with a Martensitic Microstructure. *Metals* **2024**, *14*, 1028. [CrossRef]
4. Bertocco, A.; Iannitti, G.; Caraviello, A.; Esposito, L. Lattice structures in stainless steel 17-4PH manufactured via selective laser melting (SLM) process: Dimensional accuracy, satellites formation, compressive response and printing parameters optimization. *Int. J. Adv. Manuf. Technol.* **2022**, *120*, 4935–4949. [CrossRef]
5. Callanan, J.G.; Martinez, D.T.; Ricci, S.; Derby, B.K.; Hollis, K.J.; Fensin, S.J.; Jones, D.R. Spall strength of additively repaired 304L stainless steel. *J. Appl. Phys.* **2023**, *134*, 245102. [CrossRef]
6. Ricci, S.; Testa, G.; Iannitti, G.; Ruggiero, A.; Bonora, N. On The Role of Constitutive Modeling and Computational Parameters in the Numerical Simulation of Dynamic Tensile Extrusion Test. *J. Dyn. Behav. Mater.* **2022**, *8*, 453–472. [CrossRef]
7. Ricci, S.; Iannitti, G.; Testa, G.; Sgambetterra, M.; Zucca, G.; Ruggiero, A.; Gentile, D.; Bonora, N. High-Rate Characterization of L-PBF AlSi10Mg under Impact Conditions. *J. Dyn. Behav. Mater.* **2024**, 1–13. [CrossRef]
8. Esposito, L.; Testa, G.; Bertocco, A.; Bonora, N. Creep modeling of 9–12% Cr ferritic steels accounting for subgrain size evolution. In Proceedings of the Pressure Vessels and Piping Conference, Prague, Czech Republic, 15–20 July 2018; American Society of Mechanical Engineers: New York, NY, USA, 2018; Volume 51678, p. V06AT06A056.
9. Esposito, L.; Bonora, N. Primary creep modeling based on the dependence of the activation energy on the internal stress. *J. Press. Vessel Technol.* **2012**, *134*, 061401. [CrossRef]
10. Lombardi, P.; Cipolla, L.; Folgarait, P.; Bonora, N.; Esposito, L. New time-independent formulation for creep damage in polycrystalline metals and its specialisation to high alloy steel for high-temperature applications. *Mater. Sci. Eng. A* **2009**, *510*, 214–218. [CrossRef]

11. Gentile, D.; Persechino, I.; Bonora, N.; Iannitti, G.; Carlucci, A. Use of Circumferentially Cracked Bar sample for CTOD fracture toughness determination in the upper shelf regime. *Frat. Integrità Strutt.* **2014**, *8*, 252–262. [CrossRef]
12. Esposito, L.; Gentile, D.; Bonora, N. Investigation on the Weibull parameters identification for local approach application in the ductile to brittle transition regime. *Eng. Fract. Mech.* **2007**, *74*, 549–562. [CrossRef]
13. Bonora, N.; Ruggiero, A.; Testa, G.; Iannitti, G.; Gentile, D. Dynamic Crack Tip Opening Displacement (DCTOD) as governing parameters for material fragmentation. *J. Phys. Conf. Ser.* **2014**, *500*, 112009. [CrossRef]
14. Wöhler, A. Wöhler's experiments on the strength of metals. *Engineering* **1867**, *4*, 160–161.
15. Wohler, A. Wohler's Experiments on the Fatigue of Metals. *Engineering* **1871**, *11*, 199–200.
16. Bassoli, E.; Denti, L.; Comin, A.; Sola, A.; Tognoli, E. Fatigue behavior of as-built L-PBF A357. 0 parts. *Metals* **2018**, *8*, 634. [CrossRef]
17. Tang, L. Maintenance and inspection of fiber-reinforced polymer (FRP) bridges: A review of methods. *Materials* **2021**, *14*, 7826. [CrossRef]
18. Linderov, M.; Brilevsky, A.; Merson, D.; Danyuk, A.; Vinogradov, A. On the Corrosion fatigue of magnesium alloys aimed at biomedical applications: New insights from the influence of testing frequency and surface modification of the alloy ZK60. *Materials* **2022**, *15*, 567. [CrossRef] [PubMed]
19. Campbell, G.S. A note on fatal aircraft accidents involving metal fatigue. *Int. J. Fatigue* **1981**, *3*, 181–185. [CrossRef]
20. Campbell, G.; Lahey, R. A survey of serious aircraft accidents involving fatigue fracture. *Int. J. Fatigue* **1984**, *6*, 25–30. [CrossRef]
21. Pelegatti, M.; Lanzutti, A.; Salvati, E.; Srnec Novak, J.; De Bona, F.; Benasciutti, D. Cyclic plasticity and low cycle fatigue of an AISI 316L stainless steel: Experimental evaluation of material parameters for durability design. *Materials* **2021**, *14*, 3588. [CrossRef] [PubMed]
22. Matikas, T. A high-cycle fatigue apparatus at 20 kHz for low-cycle fatigue/high-cycle fatigue interaction testing. *Fatigue Fract. Eng. Mater. Struct.* **2001**, *24*, 687–697. [CrossRef]
23. Wu, Q.; Tan, B.; Pang, J.; Shi, F.; Jiang, A.; Zou, C.; Zhang, Y.; Li, S.; Zhang, Y.; Li, X.; et al. Low-Cycle Fatigue Damage Mechanism and Life Prediction of High-Strength Compacted Graphite Cast Iron at Different Temperatures. *Materials* **2024**, *17*, 4266. [CrossRef] [PubMed]
24. Rajesh, S.; Saravanan, N. Design and Fabrication of Low Cost Fatigue Test Rig. *Imp. J. Interdiscip. Res.* **2016**, *2*, 684–688.
25. Van Hooreweder, B.; Moens, D.; Boonen, R.; Sas, P. Design and simulation of a novel multi-axial fatigue test rig. *Exp. Mech.* **2012**, *52*, 513–524. [CrossRef]
26. Nogueira, R.; Meggiolaro, M.; Castro, J. COBEM-2017-1824: A Fast Rotating Bending Fatigue Test Machine. In Proceedings of the 24th ABCM International Congress of Mechanical Engineering, Curitiba, PR, Brazil, 3–8 December 2017.
27. Gbasouzor, A.; Okeke, O.; Chima, L. Design and characterization of a fatigue testing machine. In Proceedings of the World Congress on Engineering and Computer Science, San Francisco, CA, USA, 23–25 October 2013; Volume 1.
28. Kattimani, M.A.; Khatib, M.I.; Ghori, M.M.; Sajjad, M.; Jahangir, S.; Baqtaiyan, H.; Sadiq, M. Design and fabrication of fatigue testing machine. *Int. J. Sci. Res. Sci. Eng. Technol.* **2020**, *7*, 295–304. [CrossRef]
29. Banavasi, S.M.; Ravishankar, K.; Padmayya, S. A Review on Design and Fabrication of Fatigue Testing Machine. *Int. J. Nov. Res. Dev.* **2018**, *3*, 5–14.
30. Ghielmetti, C.; Ghelichi, R.; Guagliano, M.; Ripamonti, F.; Vezzù, S. Development of a fatigue test machine for high frequency applications. *Procedia Eng.* **2011**, *10*, 2892–2897. [CrossRef]
31. Ricci, S.; Pagano, A.; Ceccacci, A.; Iannitti, G.; Bonora, N. Investigation on the Monotonic and Cyclic Behavior of Additively Manufactured TPU. *Eng. Proc.* 2024, *under review*.
32. Testa, G.; Esposito, L.; Ceccacci, A.; Iannitti, G.; Bonora, N. Innovative design and prototyping of reconfigurable run-flat tire. *Eng. Proc.* 2024, *under review*.
33. Previati, G.; Kaliske, M. Crack propagation in pneumatic tires: Continuum mechanics and fracture mechanics approaches. *Int. J. Fatigue* **2012**, *37*, 69–78. [CrossRef]
34. Major, Z.; Feichter, C.; Steinberger, R.; Lang, R. The test frequency dependence of the fatigue behavior of elastomers. In *Fracture of Nano and Engineering Materials and Structures, Proceedings of the 16th European Conference of Fracture, Alexandroupolis, Greece, 3–7 July 2006*; Springer: Dordrecht, The Netherlands, 2006; pp. 777–778.